Lattice Dynamics of Molybdenum and Chromium

B. P. Singh, L. P. Pathak, and M. P. Hemkar
Department of Physics, University of Allahabad, Allahabad-211002, India

Z. Naturforsch. **35a**, 230–235 (1980); received November 9. 1979

The frequency-wave vector dispersion relations, the frequency spectrum, the Debye temperature, the temperature dependence of the Debye-Waller factor and the mean square displacements of the atoms molybdenum and chromium, the metals for which long range forces are also important, have been computed on the basis of the extended improved Fielek model for BCC transition metals. The model considers, for the first time the d shell-d shell central interactions upto next-nearest-neighbours. The calculated results show a satisfactory agreement with the available experimental data.

1. Introduction

During the last two decades a number of phenomenological models [1–5] have been proposed for a priori calculations of the lattice vibrational properties of cubic metals. These models are fairly good for the lattice dynamical study of simple metals but do not yield equally good results for non simple metals. Fielek [6] has proposed a new lattice dynamical model for the study of non simple metals. In this model, the atoms are assumed to be composed of three entities: (i) the conduction electrons spread through out the solid, (ii) a shell of outermost d electrons and (iii) the ion core composed of the nucleus plus the remaining core electrons which move rigidly with the nucleus. We have applied this simple but powerful technique in the study of phonon dispersion relations of noble [7] and FCC and BCC transition [8, 9] metals. The results obtained were not very satisfactory. Recently we have proposed an improved Fielek model [10] for FCC transition metals by incorporating the next-nearest neighbours d shell-d shell central interactions and applied it quite successfully in studying the phonon dispersion curves of palladium and platinum and the ideal electrical resistivity and phonon dispersion relations of noble metals [11]. More recently, we have extended this model for BCC transition metals and computed the dispersion of lattice waves in α-iron and tungsten [12]. The results obtained were in fairly good agreement with the experimental data and were far better than those reported earlier on the basis of different lattice dynamical models.

In the present paper, to prove the adequacy of this extended model, we are reporting here the phonon dispersion curves, vibration spectra, the temperature variation of the Debye temperature and the Debye-Waller factor, and the mean square displacement of atoms in molybdenum and chromium.

2. Theory

The secular equation determining the angular frequencies of normal modes of vibration in a cubic crystal may be written as

$$|D(\boldsymbol{q}) - m\,\omega^2 I| = 0\,, \tag{1}$$

where $\boldsymbol{q}$ is the phonon wave vector restricted to the first Brillouin zone (BZ), m is the mass of the atom and I is the unit matrix of order three. The expressions for two typical elements of the dynamical matrix $D(\boldsymbol{q})$ are found to be

$$D_{11}(\boldsymbol{q}) = -\tfrac{8}{3}\alpha_1(1 - C_1C_2C_3) - 4\alpha_2 S_1^2 - K + K^2/N\,. \tag{2a}$$

$$D_{12}(\boldsymbol{q}) = -\tfrac{8}{3}\alpha_1 S_1S_2C_3\,, \tag{2b}$$

where

$$C_i = \cos(a\,q_i)\,,$$
$$S_i = \sin(a\,q_i);\quad i = 1, 2, 3,$$

"a" being the semi-lattice parameter, N can be evaluated from the determinant

$$|D'(\boldsymbol{q}) - NI| = 0\,. \tag{3}$$

The two typical elements of this secular determinant are

$$D'_{11}(\boldsymbol{q}) = \tfrac{8}{3}\beta_1(1 - C_1C_2C_3) + 4\beta_2 S_1^2 + K - A'G(\boldsymbol{q})\,, \tag{4a}$$

$$D'_{12}(\boldsymbol{q}) = \tfrac{8}{3}\beta_1 S_1S_2C_3 - A'G(\boldsymbol{q})\,. \tag{4b}$$

Reprint requests to B. P. Singh, Department of Physics, University of Allahabad, 13-D/2, Muir Road, Rajapur, Allahabad – 211002.

0340-4811 / 80 / 0200-0230 $ 01.00/0. — Please order a reprint rather than mak ing your own copy.

The solutions for six unknowns, viz. α_1, α_2, β_1, β_2, K and A' are discussed at length elsewhere [12].

An exponential factor e^{-2W}, often referred to as the Debye-Waller factor, enters into a large number of solid state phenomena such as Mössbauer effect, neutron scattering, mean square displacement of atoms, thermal and electrical resistivity etc. of solids. The contribution to the DW factor ($2W$) consists of two parts:

(i) the one which depends upon phonons and is obtained from the knowledge of the whole vibration spectra. Following James [13] this contribution is expressed as

$$2W' = \frac{2}{3}\,\frac{h}{mN}\left(\frac{\sin\theta}{\lambda}\right)^2 \cdot \sum_{q,j} (\nu_{q,j})^{-1} \coth(h\,\nu_{q,j}/2k_B T), \tag{5}$$

where the terms used have their usual meaning.

(ii) The other one due to the central part of the BZ corresponding to $\boldsymbol{q} \to 0$ and evaluated in the Debye approximation as

$$2W'' = \frac{16a^3}{3m}\,[D(C_L) + 2D(C_T)]\left(\frac{\sin\theta}{\lambda}\right)^2, \tag{6}$$

where C_L and C_T correspond to the average velocities for the longitudinal and transverse phonons, respectively, in the region $\boldsymbol{q} \to 0$ and $D(C)$ can be evaluated from

$$D(C) = P/x \int_0^x \frac{t\,dt}{e^t - 1} + \frac{1}{4}\,P x\,. \tag{7}$$

Here $P = 2\pi k_B T\, q_{\max}/C^2$, $x = h\, q_{\max}\, C/k_B T$,

$$t = \frac{hqC}{2\pi k_B T} \quad \text{and} \quad q_{\max} = \frac{\pi}{10a}(3/2\pi)^{1/3}\,.$$

Thus the total DW factor ($2W$) is

$$2W = 2W' + 2W''\,. \tag{8}$$

In the harmonic approximation, the mean square displacement of atoms $\overline{U^2}$ is given by

$$\overline{U^2} = \frac{3}{16\pi^2}\left(\frac{\lambda}{\sin\theta}\right)^2 (2W)\,. \tag{9}$$

3. Numerical Computation

The phonon dispersion curves of molybdenum and chromium are calculated from the secular Eq. (1) along the three highly symmetric directions. The experimental input parameters and the calculated values of the force constants are listed in Table 1 and Table 2, respectively.

The frequency distribution function $G(\nu)$ has been computed by Blackmann's sampling method. In order to get fairly a large number of frequencies, the translational vector in reciprocal space is

Table 1. Input parameters.

Metal	Elastic constants ($\times 10^{11}$ dyn cm^{-2})			Lattice constant	Zone boundary frequencies (THz)		
	C_{11}	C_{12}	C_{44}	$2a$ (Å)	$\nu_L(100)$	ν_{T_2} $(\frac{1}{2}\,\frac{1}{2}\,0)$	ν_L $(\frac{1}{2}\,\frac{1}{2}\,0)$
Molybdenum [a]	44.077	17.243	12.165	3.1468	5.51	4.67	8.22
Chromium [b]	35.00	6.78	10.08	2.8792	7.554	5.8	9.5

[a] F. H. Featherston and J. R. Neighbours, Phys. Rev. **130**, 1324 (1963).

[b] D. I. Bolef and J. de Klerk, Phys. Rev. **129**, 1063 (1963).

Table 2. Output values of force constants (in units of 10^3 dyn cm^{-1}).

Metal	α_1	α_2	β_1	β_2	K	A'
Molybdenum	− 71.9092	− 38.7565	14.4880	− 3.4641	− 124.1429	80.4750
Chromium	− 43.9698	− 40.3576	0.4363	− 0.2679	− 3.48	− 34.7491

divided into 20 equal parts so as to give a grid of 8000 equally spaced points inside the first BZ. On account of the symmetry properties of the lattice and Born's cyclic boundary condition, these 8000 points reduce to 256 non-equivalent points including the origin, lying within the 1/48th irreducible sector of the first BZ. The 24000 frequencies corresponding to 8000 points are calculated from (1).

From the knowledge of frequency spectra, one can easily calculated the lattice specific heat at constant volume from the relation

$$C_v = k_B \int_0^{\nu_m} x^2\, e^x/(e^x - 1)^2\, G(\nu)\, d\nu\,, \qquad (10)$$

where

$$x = h\,\nu/k_B T \quad \text{and} \quad \int_0^{\nu_m} G(\nu)\, d\nu = 3N\,, \qquad (11)$$

N being the number of atoms per gram molecule.

The results obtained for the specific heat (C_v) are expressed in terms of the effective Debye temperature Θ after substracting the electronic specific heat contribution from the experimental C_v values. For this purpose, the coefficients of the electronic specific heat for molybdenum and chromium have been taken to be 50×10^{-5} and 3.6×10^{-5} cal (gram atom)$^{-1}$ deg^{-2}, respectively as reported by Clusius and Franzosini [14] and Feldman [15].

Using the computed frequency spectra, the temperature variation of the DW factor is studied with the help of (5)—(8), and the corresponding mean square displacement of atoms is evaluated from (9). The calculated DW factor has been compared in terms of a temperature parameter Y which is defined as

$$Y = (\lambda/\sin\theta)^2 \log_{10} e\,[2\,W_{T_0} - 2\,W_T]\,, \qquad (12)$$

where W_{T_0} and W_T are the DW exponents at the temperatures T_0 and T and are quite independent of λ and θ. The DW exponent is directly assessed from the measurements of X-ray intensities of Bragg reflections as

$$I_T/I_0 = \exp(-2\,W_T)/\exp(-2\,W_{T_0})\,, \qquad (13)$$

where I_T and I_0 are the X-ray intensities at the temperatures T and T_0, respectively. From (12) and (13) we obtain

$$Y = (\lambda/\sin\theta)^2 \log_{10}(I_T/I_0)\,. \qquad (14)$$

4. Results and Discussion

Molybdenum. The calculated phonon dispersion curves are plotted in Fig. 1 along with the experimental values of Woods and Chen [16]. As is quite evident from the figure that our calculated curves agree well with the experimental data except for the Δ_L branch for large values of the wave vector and the Σ_{T_1} branch as a whole.

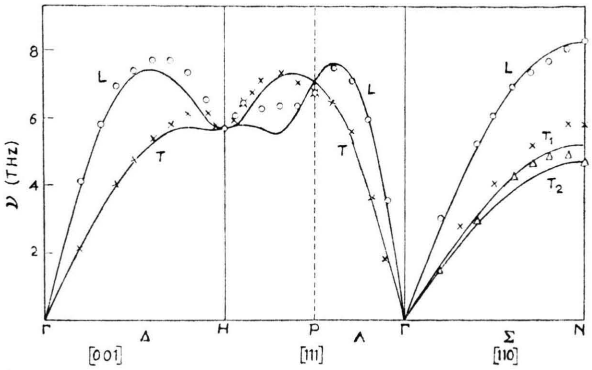

Fig. 1. Dispersion curves along the symmetry directions for molybdenum. Solid curves from the present calculations. Experimental points (○, ×, △) from Woods amd Chen [16].

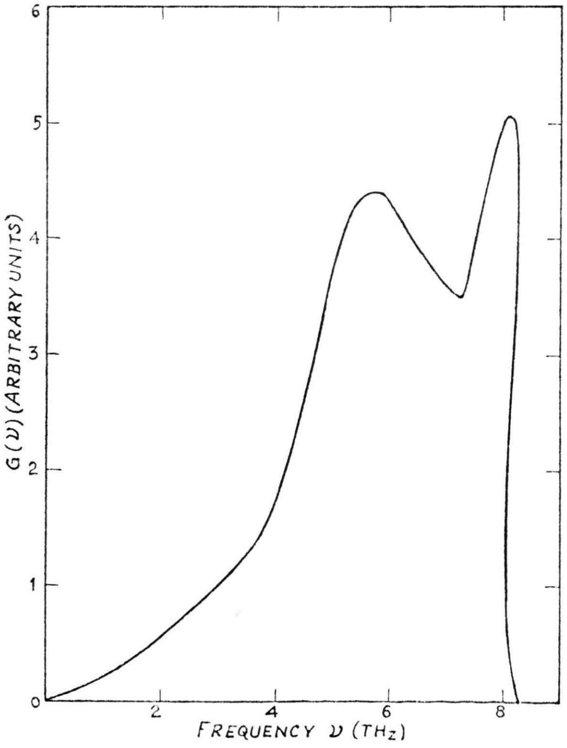

Fig. 2. Frequency spectrum of molybdenum.

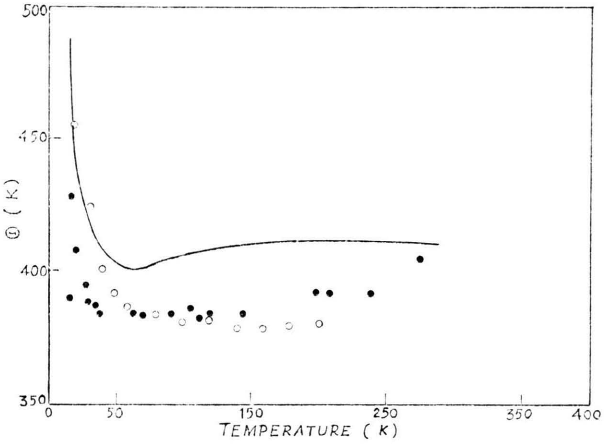

Fig. 3. Temperature variation of the equivalent Debye temperature of molybdenum. Solid curve from the present calculations. Experimental points (● ● ●) from Simon and Zeidler [17] and (○ ○ ○) from Clusius and Franzosini [14].

The calculated frequency spectrum is plotted in Figure 2. Experimental observations, being absent, no conclusion can be drawn as to the adequacy of the theoretical curve. Using this spectrum, the calculated specific heat is expressed in terms of the Debye temperature in Fig. 3 along with the experimental values of Clusius and Franzosini [14] and that of Simon and Zeidler [17]. The calculated $\Theta - T$ curve agrees well at lower temperatures with the experimental data of Clusius and Franzosini but does not agree with the data of Simon and Zeidler throughout the temperature range.

Korsunskii [18] measured the intensity ratio I_{291}/I_T of the crystal for the (232) and (322) reflection planes in the temperature range 100—400 K. His results are plotted in Fig. 4 along with our theoretical values for Y and $\overline{U^2}$ with 291 K as reference temperature. It is evident from the figure that our theoretical curves approach the experimental value of the (322) reflecting plane.

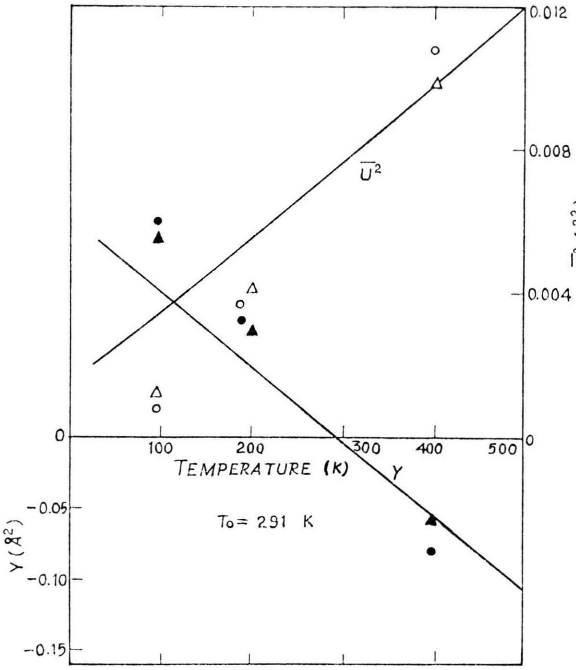

Fig. 4. Temperature variation of Y and $\overline{U^2}$ of molybdenum. Solid curves from the present calculations. Experimental points ○ ○ (232 plane) and △▲ (322 plane) from Korsunskii [18].

Chromium. Shaw and Muhlestein [19] have measured the detailed phonon dispersion curves at room temperature by means of thermal neutron scattering. Their dispersion curves show four regions of anomalous behaviour which are related with the departure of the Fermi surface from sphericity. The calculated phonon dispersion curves are plotted in Fig. 5 along with the experimental values [19]. Our curves are in fairly good agreement. The crossing over of the Λ_L and Λ_T branches in the P-H region, which had never been obtained by any lattice dynamical model, is the most salient feature of the present calculations. The slight deviations of the theoretical curves from the experimental values are generally in the anomalous

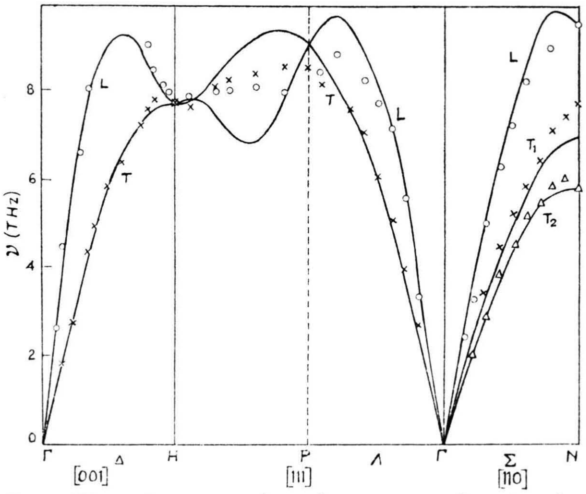

Fig. 5. Dispersion curves along the symmetry directions for chromium. Solid curves from the present calculations. The experimental points (○, ×, △) are of Shaw and Muhlestein [19].

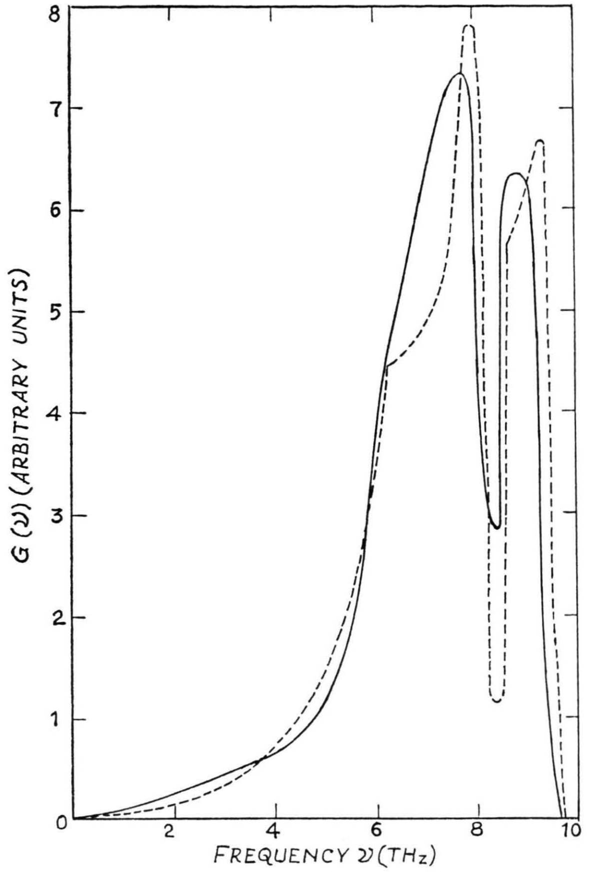

Fig. 6. Frequency spectrum of chromium. Solid curve from the present calculations. Experimental curve (----) from Shaw and Muhlestein [19].

behaviour regions because in the present computations the Fermi surface is considered as spherical.

The theoretical vibration spectrum for chromium is shown in Fig. 6 along with the experimental values of Shaw and Muhlestein [19]. It is seen from the figure that our calculated $G(\nu)$ values agree in their broad features with the experimental spectrum. The calculated spectrum has two prominent peaks, the lower frequency peak being more intense. The temperature variation of the Debye temperature is shown in Fig. 7 together with the experimental values of Clusius and Franzosini [20] and Heiniger's [21] estimated values. The calculated curve agrees well with the estimated values of Heiniger throughout the whole temperature range but does not match with the experimental data of Clusius and Franzosini.

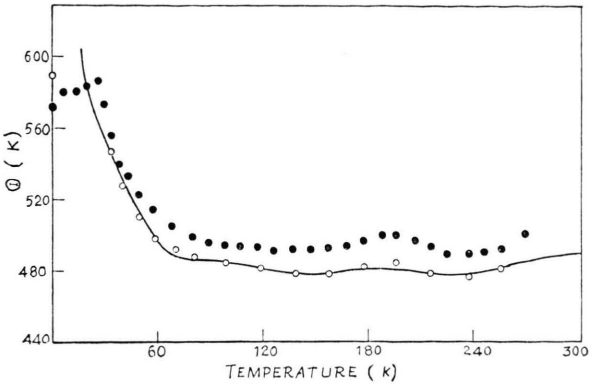

Fig. 7. Temperature variation of the equivalent Debye temperature of chromium. Solid curve from the present calculations. Experimental points (● ● ●) from Clusius and Franzosini [20] and (○ ○ ○) as estimated by Heiniger [21].

The calculated $Y - T$ and $\overline{U^2} - T$ curves are compared with the experimental results of Wilson et al. [22] in Fig. 8 with T_0 (298 K) as reference temperature. A reasonable agreement between theory and experiment is observed.

The discrepancies may, however, be attributed to the neglect of:

(i) the temperature variation of elastic constants and normal modes frequencies,

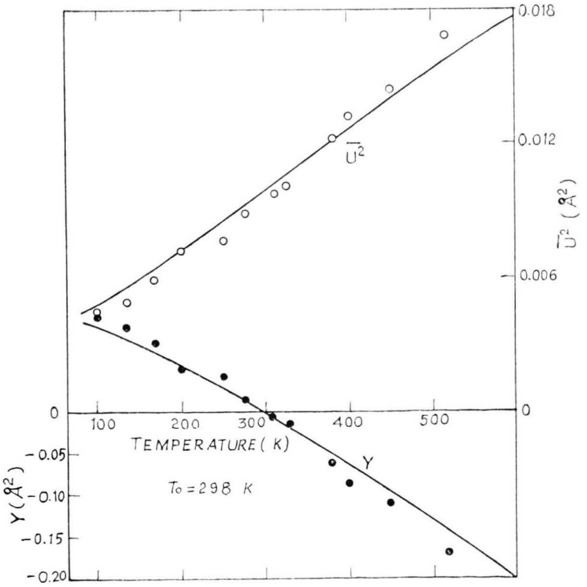

Fig. 8. Temperature variation of Y and U^2 of chromium. Solid curves from the present calculations. Experimental points (○ ●) from Wilson et al [22].

(ii) the anharmonicity effects [23, 24],
(iii) the ion core-conduction electrons interaction,
(iv) the flexibility of d-orbitals.

As the things stand, it emerges from the present study that various lattice dynamical properties of non simple metals are adequately expressed with the present model.

Acknowledgement

The authors are very grateful to Professor Vachaspati for providing adequate facilities in the department. One of us (B.P.S.) extends his sincere thanks to the University Grants Commission, New Delhi, for the award of "Teacher Fellowship".

[1] A. B. Bhatia, Phys. Rev. **97**, 363 (1965).
[2] J. de Launay, Solid State Physics, Academic New York **2**, 276 (1956).
[3] P. K. Sharma and S. K. Joshi, J. Chem. Phys. **39**, 2633 (1963).
[4] K. Krebs, Phys. Rev. **138A**, 143 (1965).
[5] L. Cheveau, Phys. Rev. **199**, 496 (1968).
[6] B. L. Fielek, J. Phys. F **5**, 17 (1975).
[7] B. P. Singh, L. P. Pathak, and M. P. Hemkar, Acta Phys. Poln. **54A**, 207 (1978).
[8] B. P. Singh, L. P. Pathak, and M. P. Hemkar, J. Phys. Soc. Japan, **45**, 484 (1978).
[9] B. P. Singh and M. P. Hemkar, Acta Phys. Acad. Sci. Hung. (1979), in print.
[10] B. P. Singh, L. P. Pathak, and M. P. Hemkar, J. Phys. F **8**, 2493 (1978).
[11] B. P. Singh and M. P. Hemkar, Z. Naturforsch. **34a**, 310 (1979).
[12] B. P. Singh and M. P. Hemkar, Acta Phys. Poln. **56A**, (1979).
[13] R. W. James, The Optical Principle of the Diffraction of X-rays Bell and Sons, London 1954.
[14] K. Clusius and P. Franzosini, Z. Naturforsch. **14a**, 99 (1959).
[15] J. L. Feldman, Phys. Rev. **B1**, 448 (1970).
[16] A. D. B. Woods and S. H. Chen, Solid State Commun. **2**, 233 (1964).
[17] F. Simon and W. Zeidler, Z. Phys. Chem. Frankfurt **123**, 387 (1962).
[18] M. I. Korsunskii, Sov. Phys. Solid State **13**, 413 (1971).
[19] W. M. Shaw and L. D. Muhlestein, Phys. Rev. **4B**, 969 (1971).
[20] K. Clusius and P. Franzosini, Z. Naturforsch. **17a**, 522 (1962).
[21] F. Heiniger, Phys. Kondens. Mater. **5**, 285 (1966).
[22] R. H. Wilson, E. F. Skelton, and J. L. Katz, Acta Cryst. **21**, 635 (1966).
[23] B. T. M. Willis, Acta Cryst. **A25**, 277 (1969).
[24] G. A. Wolfe and B. Goodman, Phys. Rev. **178**, 1171 (1969).